



CELL WALL SYMPOSIUM



## New Zealand Journal of Forestry Science

39 (2009) 251-257

<http://nzjfs.scionresearch.com>



---

### Nature's Nanocomposites: A New Look at Molecular Architecture in Wood Cell Walls<sup>†</sup>

Stefan J. Hill<sup>1,\*</sup>, Robert A. Franich<sup>1</sup>, Paul T. Callaghan<sup>2</sup> and Roger H. Newman<sup>1</sup>

<sup>1</sup>Scion, Private Bag 3020, Rotorua 3046, New Zealand

<sup>2</sup>MacDiarmid Institute for Advanced Materials and Nanotechnology, Victoria University of Wellington, PO Box 600, Wellington, New Zealand

(Received for publication 31 October 2008; accepted in revised form 16 October 2009)

\*corresponding author: [stefan.hill@scionresearch.com](mailto:stefan.hill@scionresearch.com)

---

#### Abstract

A widely-accepted model for the molecular architecture of wood fails to account for the stick-slip deformation process, in which wet wood shows permanent plastic deformation without significant mechanical damage. A proposed model interposes a layer of water molecules between cellulose microfibrils and the surrounding matrix. Results from proton spin diffusion, monitored via <sup>13</sup>C NMR signal strengths, supported the new model. *Pinus radiata* D.Don latewood was soaked in D<sub>2</sub>O and a timescale of 10 ms was measured for proton spin diffusion between cellulose and glucomannan. This observation was interpreted in terms of a layer of D<sub>2</sub>O molecules creating a spin-diffusion barrier between the microfibrils and the matrix.

**Keywords:** cell walls; cellulose; glucomannan; lignin; nuclear magnetic resonance; *Pinus radiata*

<sup>†</sup>Based on a paper presented at the 3rd Joint New Zealand – German Symposium on Plant Cell Walls, 13-15 February 2008, Auckland, New Zealand

#### Introduction

Keckes et al. (2003) drew attention to a remarkable property of wet wood. When stretched beyond its elastic limit, wet wood shows irreversible deformations and yet it does not flow as plastics do. As soon as the excess stress is released, the original stiffness is restored. In other words, wet wood shows permanent plastic deformation without significant mechanical damage. This behaviour is known as “stick-slip” deformation, and has been compared to Velcro<sup>®</sup> mechanics (Kretschmann, 2003). When Velcro<sup>®</sup> is deformed beyond a yield point, the hooks open and slip until the excess stress is released. The hooks then close on a different set of loops. The outstanding question is: what components of the wood cell wall

correspond to the hooks and loops of Velcro<sup>®</sup>? The stick-slip deformation process challenges our current understanding of the molecular architecture of wood. In this paper, we discuss the possibility that water molecules play an important role in stick-slip deformation. We also present the results from scoping experiments that explored new ways of testing the role of water molecules in such structures.

The earliest model of a wood cell wall showed microfibrils of crystalline cellulose wound in helical springs and embedded in an amorphous matrix of hemicelluloses and lignin (Mark, 1965; Cowdrey & Preston, 1965; Cowdrey & Preston, 1966; Frey-

Wyssling, 1968). This model provided satisfactory foundations for calculations of the elastic properties of dry wood (Cave, 1968), but it did not seem adequate to explain the strength of wet wood. Page (1976) addressed this problem by suggesting that hemicellulose chains act as coupling agents between cellulose microfibrils and lignin. Ruel et al. (1978) incorporated this idea in a three-phase model for a wood cell wall, with partial segregation of the lignin-hemicellulosic matrix into a hemicellulose-rich region adjacent to the cellulose and a lignin-rich region further away. Partial segregation of hemicellulose from lignin has been retained in more recent models (Bergander & Salmén, 2002; Gravitis, 2006). The idea of partial segregation has been refined by distinguishing between the two major hemicelluloses, i.e. glucomannan and xylan. Dynamic infra-red spectroscopy indicated close cooperation between glucomannan and cellulose molecules, but no mechanical interaction between xylan and cellulose (Åkerholm & Salmén, 2001). A revised model (Figure 1) is not greatly different from that proposed by Page (1976), except for the different locations of glucomannan and xylan.

The model represented in Figure 1 accounts for wet strength, as required by Page (1976), but it requires further refinement to account for the stick-slip deformation reported by Keckes et al. (2003). A single hydrogen bond is an order of magnitude weaker than a single covalent C-O bond linking two glucosyl structural units in cellulose, but when the load is distributed over numerous hydrogen bonds, as in Figure 1, it seems unlikely that a glucomannan chain would become detached from a cellulose microfibril by shear stress alone (Altaner & Jarvis, 2008). If the glucomannan chains follow a more winding path between cellulose microfibrils, they might be more readily peeled under shear stress (Altaner & Jarvis, 2008). Alternatively, the glucomannan chains might remain attached to cellulose microfibrils and the changes associated with stick-slip deformation might occur within the lignin-hemicellulosic matrix (Sedighi-Gilani & Navi, 2007).

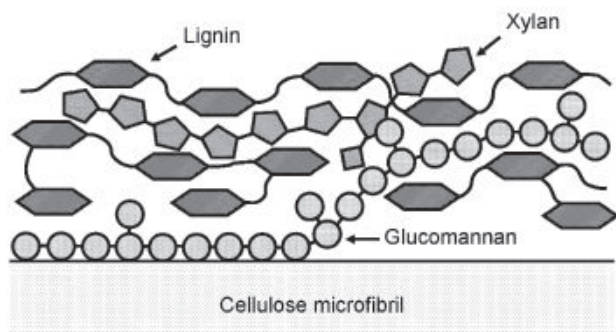


FIGURE 1: A model for the interface between a cellulose microfibril and the adjacent matrix, showing a glucomannan chain locking the components together as suggested by Page (1976).

Another model (Figure 2) shows a layer of water molecules attached to the surface of the cellulose microfibril. This idea was mentioned by Hansen and Bjorkman (1998), but those authors did not offer any experimental evidence. Figure 2 differs from Figure 1 in an important detail: the interaction between glucomannan and cellulose is confined to a short segment of the chain between structural units bearing side groups. Softwood glucomannans bear galactosyl and acetyl side groups. Laffend and Swenson (1968) showed that the degree of acetylation of glucomannan influences the strength of sorption onto cellulose. Newman (1992) used solid-state NMR spectroscopy to show that the acetylated segments of glucomannan in Douglas-fir (*Pseudotsuga menziesii* (Mirbel) Franco) wood are intimately mixed with lignin but distant from cellulose. Hansen and Bjorkman (1998) pointed out that the solubility parameter for an acetylated hemicellulose makes it more compatible with lignin than with cellulose. The overall conclusion from these observations is that side groups provide two independent mechanisms for limiting coupling to cellulose: (1) galactosyl side groups provide steric interference, hindering contact with the surface of the cellulose; and (2) acetyl groups promote incorporation of the glucomannan in the matrix. In the model represented in Figure 2, stick-slip deformation occurs at the interface between a glucomannan segment and a layer of water molecules.

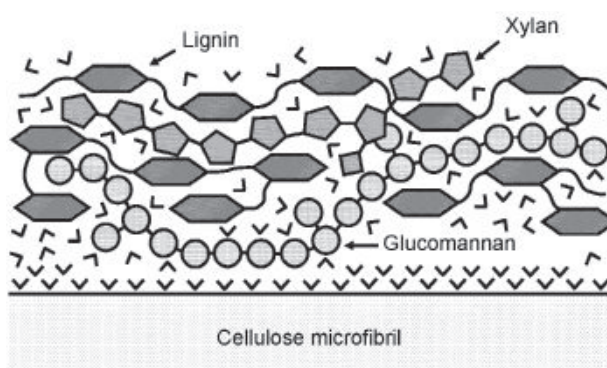


FIGURE 2: A new model for the interface between a cellulose microfibril and the adjacent matrix, showing a layer of water molecules (v symbols) adhering to the microfibril.

The representation in Figure 2 might remain valid for wood dried to an equilibrium moisture content of approximately 12% at 65% relative humidity. Below 12% moisture, we predict changes in stick-slip deformation, but do not expect those changes to be severe or pronounced. It seems more likely that the response to loading will show a continuous change as wood is dried from the green state (multiple layers of water molecules on cellulose) through low water contents (predominantly monolayers of water molecules as in Figure 2) to absolute dryness. The final monolayer of water is not removed from the cellulose microfibrils of wood until a much lower

moisture content is reached (Weatherwax, 1974). Complete removal of water would bring glucomannan into contact with cellulose, and the hydrogen bonds might not be easily broken on rehydration. There are literature references to support this idea, e.g. Klauitz et al. (1947) found that the wet strength of pulped wood fibres doubled when the fibres were dried and rewet.

We tested the new model using proton spin diffusion, a technique that is often used to characterise the nanostructure of synthetic polymers (McBrierty, 1979; Clauss et al., 2003). It is important to note that it is the spin information, not the nucleus itself, that moves through the solid matter. Each proton becomes aligned in the magnetic field of a nuclear magnetic resonance (NMR) spectrometer, in either a “spin up” or “spin down” quantised state (Figure 3). Adjacent nuclei exchange spin information through “flip-flop” interactions, so that mixing occurs according to a “random walk” process. For spin diffusion in a fibrous polymer, the mean-square distance affected after a mixing time  $t_m$  is (Chen & Schmidt-Rohr, 2006):

$$\langle x^2 \rangle = 4Dt \quad [1]$$

Here  $D$  is the diffusion coefficient. Recent experiments have indicated a value of  $D = 0.5$  nm/ms for proton spin diffusion in organic polymers (Chen & Schmidt-Rohr, 2006). In the case of pine wood, we know that the radius of a typical cellulose microfibril is approximately 1.5 nm (Nomura et al., 1972; Takada et al., 1981). Equation [1] then predicts proton spin diffusion between the core and the surface of a cellulose microfibril over  $t \approx 1$  ms. If a single glucomannan molecule is in contact with cellulose, as in Figure 1, then the radius will increase by 0.6 nm and mixing will take a little longer, perhaps  $t \approx 2$  ms. If there is an intervening layer of water ( $H_2O$ ) molecules, as in Figure 2, mixing will take even longer. If the specimen is soaked in heavy water ( $D_2O$ ), mixing will take much longer because protons and deuterons do not exchange quantised spin information through “flip-flop” interactions (Figure 3b). The presence of a barrier can, therefore, be tested by soaking wood in  $D_2O$  and measuring the time constant for spin diffusion between cellulose and glucomannan. A time constant  $t \gg 2$  ms might be taken as evidence for a barrier.

Proton spin diffusion can be detected through its influence on  $^{13}C$  NMR signal strengths. Newman (1992) and Altaner et al. (2006) described spin diffusion experiments on softwoods, using  $^{13}C$  NMR signals assigned to cellulose and lignin. In those experiments, proton spin diffusion took 20 or 25 ms to mix spin information between the two polymers. A time constant of this magnitude is consistent with clustering of microfibrils in cellulose-rich macrofibrils, surrounded by lignin-rich domains (Salmén & Fahlen, 2006; Donaldson, 2007). The proposed test for a layer of water molecules requires NMR equipment with greater sensitivity than that used by Newman

(1992), because the relevant glucomannan signal is weak. Altaner et al. (2006) used suitable equipment, but did not attempt to create a spin-diffusion barrier. Suitable equipment was recently installed at Scion, and was used in the work described here.

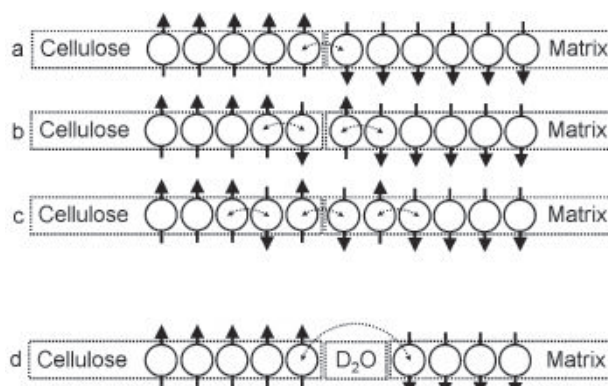


FIGURE 3: Representation of nuclear spin diffusion: (a)-(c) without a barrier; and (d) with a barrier. The segregation of “spin up” and “spin down” quantised states is greatly exaggerated. In reality, there is never more than a fractional surplus of one over the other. Double-headed arrows indicate pairs of nuclei that will exchange spin information in the next step.

## Materials and Methods

A sample of radiata pine (*Pinus radiata* D. Don) wood was collected in August 2008. Bark was removed at breast height, the exposed wood was marked to identify the bark side, and a slice approximately 2 mm thick was chiseled into a vial containing distilled water. A subsample was removed and examined using field emission scanning electron microscopy (FESEM) to determine the thickness of the latewood. This layer was then taken from the slice with a scalpel. Latewood was considered more desirable than earlywood because the relatively thick cell walls were expected to provide a satisfactory signal-to-noise ratio. Fragments were cut to dimensions  $< 1$  mm, immersed in  $D_2O$  and stirred for 1 h, moved to fresh  $D_2O$  and stirred for 4 h, and finally moved to fresh  $D_2O$  and stirred overnight. A portion weighing 96 mg was packed in a 4 mm zirconium oxide rotor with a Kel-F® cap. A random sample of eight of the fragments was examined by FESEM to confirm the absence of earlywood.

The sample was spun at 5 KHz in a 4 mm Bruker SB magic-angle spinning probe, for  $^{13}C$  NMR at 50.3 kHz using a Bruker 200 DRX spectrometer. For the standard cross-polarisation (CP) experiment, each 1.5 s pulse delay was followed by a proton preparation pulse of duration  $t_p = 5.6 \mu s$ , a 1 ms contact time and a 30 ms acquisition time. The proton transmitter power was increased to a value corresponding to a  $90^\circ$  pulse width of  $1.4 \mu s$  for proton decoupled during

$^{13}\text{C}$  data acquisition. Transients were averaged over a period of 5 h.

Spin-spin relaxation time constants  $T_{2H}$  were estimated by a nutation-CP pulse sequence (Newman, 1987) illustrated in Figure 4a. The word nutation has its roots in astronomy: the earth's rotational axis precesses in the gravitational field of the sun, and nutates in that of the moon. Likewise, nuclear magnetisation precesses in the static magnetic field of an NMR spectrometer and nutates in the weaker oscillating field generated by a radiofrequency transmitter. If the proton transmitter frequency is matched to the precession frequency, and proton magnetisation is transferred to  $^{13}\text{C}$  nuclei by CP, then a plot of  $^{13}\text{C}$  NMR signal height against the nutation pulse width  $t_n$  shows a sinusoidal oscillation damped by a time constant of  $2T_{2H}$  (Newman, 1987). In the present work, the oscillation was represented by:

$$h(t_n) = A \sin(\gamma_H B_H t_n) \exp(-0.5t_n/T_{2H}) \quad [2]$$

Here  $\gamma_H$  is the magnetogyric ratio for a proton and  $B_H$  is the magnetic field strength used for decoupling. Transients were averaged over a period of 2 h for each value of  $t_n$ .

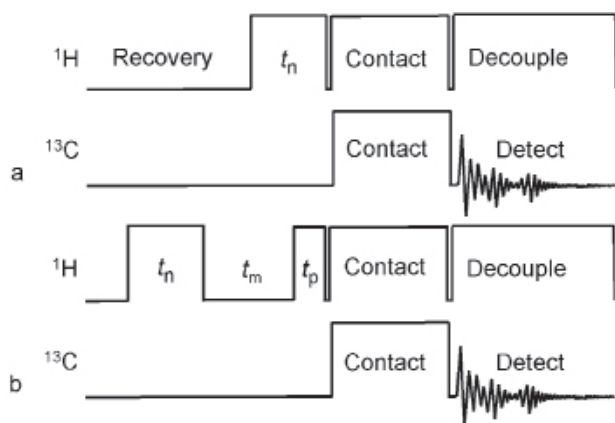


FIGURE 4: Pulse sequences for: (a) a nutation-CP experiment to measure spin-spin relaxation time constants; and (b) a nutation-diffusion-CP experiment to characterise proton spin diffusion. Subscripts n, m and p refer to nutation, mixing and preparation pulses, respectively.

Several pulse sequences have been proposed for detecting proton spin diffusion through its influence on  $^{13}\text{C}$  NMR signal strengths (Tekely et al., 1989; Schmidt-Rohr et al., 1990; Newman, 1991). We chose to use a different simpler pulse sequence, illustrated in Figure 4b, because we expected that its simplicity would minimise signal distortions caused by radiofrequency pulse imperfections. Nutation during a pulse of width  $t_n = 33.6 \mu\text{s}$  rotated the proton magnetisation through  $540^\circ$ , leaving it inverted. Spin-spin relaxation occurred during nutation, leaving proton magnetisation relatively depleted in domains with relatively short values of  $T_{2H}$ . Spin diffusion

occurred during a mixing time  $t_m$ , after which the proton magnetisation was characterised by cross-polarisation to  $^{13}\text{C}$  nuclei. Transients were averaged over a period of 5 h for each value of  $t_m$ . Peak heights were normalised relative to the height observed in standard cross-polarisation NMR spectra, i.e. those obtained with the pulse sequence represented in Figure 4a but with  $t_n$  fixed at a value corresponding to  $90^\circ$  nutation.

## Results and Discussion

A spectrum obtained with the standard  $^{13}\text{C}$  CP NMR pulse sequence is shown in Figure 5. Signal assignments follow Newman (1992) and Newman and Hemmingson (1998). Signals were selected as representative of each of three types of polymer:

- 55.8 ppm: methoxyl carbon of lignin;
- 88.9 ppm: C-4 of glucosyl structural units in the interiors of cellulose microfibrils; and
- 101.4 ppm: C-1 of mannosyl structural units in glucomannan.

A shoulder on the peak at 101.4 ppm was assigned to C-1 in the galactosyl side-chain units of glucomannan (Newman & Hemmingson, 1998). Altaner et al. (2006) used the same signals, along with signals in the range 80 ppm to 84 ppm. We avoided the latter signals because of concerns about overlapping contributions from lignin, cellulose and/or hemicelluloses.

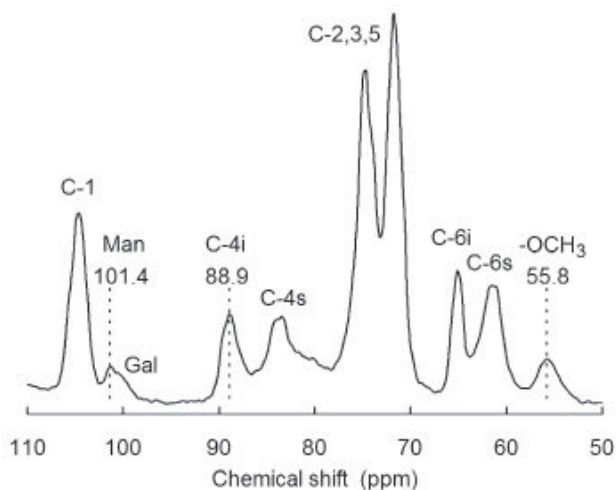


FIGURE 5: Carbon-13 NMR spectrum of never-dried *Pinus radiata* wood. Broken lines mark peaks used for signal-height measurements. Carbon numbers refer to the glucosyl structural units of cellulose. Man = mannosyl C-1 signal, Gal = galactosyl C-1 signal. Labels *i* and *s* refer to interiors and surfaces of cellulose microfibrils, respectively.

A nutation-CP experiment indicated a best-fit value of  $T_{2H} = 13 \mu\text{s}$  for glucomannan (Figure 6). Other curves (not illustrated) indicated  $T_{2H} = 10 \mu\text{s}$  and  $14 \mu\text{s}$  for cellulose and lignin, respectively. The experiments were not intended to give accurate values of  $T_{2H}$ . Obtaining an accurate value for  $T_{2H}$  that would require consideration of Gaussian or other damping functions, and the consequences of radiofrequency field inhomogeneities (Newman, 1987). All that was necessary to support the present work was to show that the values of  $T_{2H}$  were sufficiently different to allow a nutation pulse to change the relative proportions of proton magnetisation in cellulose and non-cellulosic polymers.

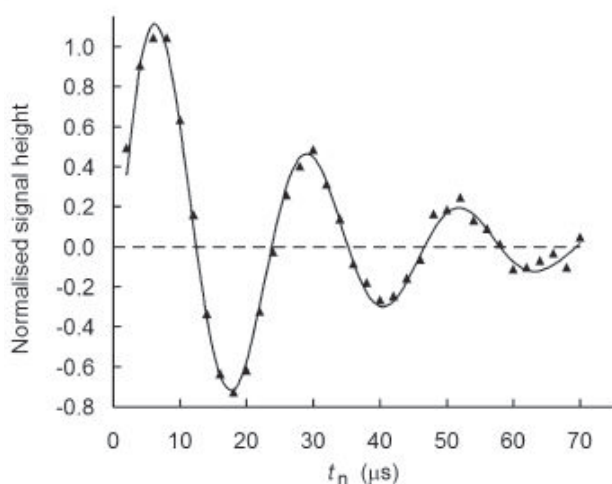


FIGURE 6: Measurement of  $T_{2H}$  by a nutation-CP experiment, using the  $^{13}\text{C}$  NMR signal at 101.4 ppm. The best-fit curve was calculated for  $T_{2H} = 13 \mu\text{s}$ .

Results from the nutation-diffusion-CP experiments (Figure 7) showed negative signal heights caused by inversion of the proton magnetisation during  $t_n$ . Normalisation of the signal height, relative to that observed in a standard CP NMR spectrum, gave a measure of relative proton magnetisation in three polymers: lignin, cellulose and glucomannan. Curves for lignin and cellulose converged after a mixing time of  $t_m = 10 \text{ ms}$ . The timescale was shorter than published values for experiments on similar samples of wood: 20 ms and 25 ms for radiata pine and Sitka spruce (*Picea sitchensis* (Bongard) Carrière), respectively (Newman, 1992; Altaner et al., 2006). Proton spin-lattice relaxation time constants  $T_{1H}$  were also shorter in this work, causing the curves in Figure 7 to rise steeply at the highest values of  $t_m$ . Differences between the three studies are not surprising, considering differences in sample preparation. In particular, wood was dried and rewetted for the earlier studies (Newman, 1992; Altaner et al., 2006), but never dried in the present work.

Figure 7 also shows that the spin-diffusion curve for the glucomannan signal was superimposed on that

for lignin, and converged with the curve for cellulose after a mixing time of  $t_m = 10 \text{ ms}$ . Our results were consistent with the model illustrated in Figure 2, which places glucomannan on the matrix side of a spin-diffusion barrier. The results were not consistent with close contact at the interface, i.e. the model illustrated in Figure 1. Spin diffusion between cellulose and adhering glucomannan segments would require a much shorter timescale of  $t_m \approx 2 \text{ ms}$ , as discussed in the Introduction. The data points for glucomannan showed more scatter than those for lignin or cellulose, so it was not possible to reject a version of Figure 1 in which the bulk of the glucomannan is embedded in the matrix, and just short segments adhere to cellulose. More work is required to determine an upper limit on the proportion of glucomannan that might adhere to cellulose.

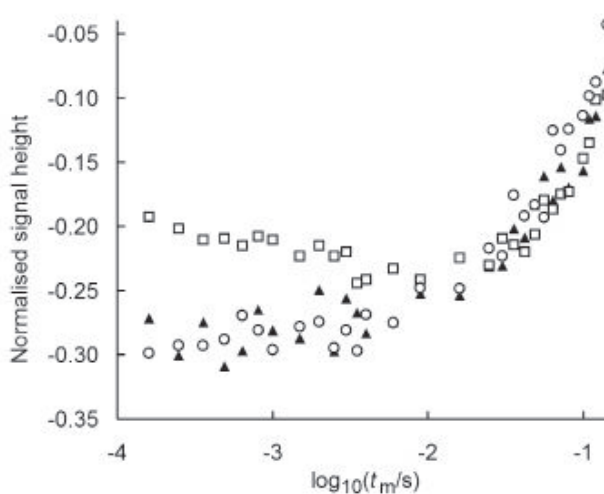


FIGURE 7: Results from a nutation-diffusion-CP experiment. Signal heights were measured at 55.8 ppm (lignin, circles), 88.9 ppm (cellulose, squares), and 101.4 ppm (glucomannan, triangles), and normalised relative to a spectrum obtained by the standard CP sequence.

We did not repeat measurements on a sample soaked in  $\text{H}_2\text{O}$ , because the interpretation would be confused by the fact that  $\text{H}_2\text{O}$  has a large number of protons per unit weight, relative to cell-wall polymers. Those protons provide a large reservoir of nuclear magnetisation, so spin diffusion curves are likely to be dominated by diffusion between polymers and water, rather than diffusion from one polymer to another. Nevertheless, a published study of proton spin diffusion of wood soaked in  $\text{H}_2\text{O}$  provides a few insights (Altaner et al., 2006). In particular, the curves for microfibril-interior and microfibril-surface cellulose converged after  $t \approx 4 \text{ ms}$ . This is longer than the value of  $t_m \approx 1 \text{ ms}$  calculated in the Introduction, but close enough to show that the theory is reasonable. Altaner et al. (2006) also measured the height of the glucomannan signal at 101 ppm. The curve was not superimposed on that

for lignin, and converged on the curve for microfibril-surface cellulose after  $t_m \approx 10$  ms. This timescale was taken as evidence for partial segregation of glucomannan from the lignin-hemicellulosic matrix.

## Conclusion

The results described here are consistent with the presence of a layer of water molecules between the cellulose microfibrils and the surrounding matrix. This model is also consistent with the stick-slip deformation process described by Keckes et al. (2003), whereby hydrogen bonding between the water molecules and matrix polymers could provide the "hooks" and "loops" required by the stick-slip model.

Removal of the layer of water molecules is expected to collapse the matrix onto the cellulose microfibrils. More work is needed to explore the consequences of this collapse, and the possibility that it might be no more than partly reversible when the wood is rewetted.

## References

- Åkerholm, M., & Salmén, L. (2001). Interactions between wood polymers studied by dynamic FT-IR spectroscopy. *Polymer*, *42*, 963-969.
- Altaner, C., Apperley, D. C., & Jarvis, M. C. (2006). Spatial relationships between polymers in Sitka spruce: proton spin-diffusion studies. *Holzforschung*, *60*, 665-673.
- Altaner, C. M., & Jarvis, M. C. (2008). Modelling polymer interactions of the 'molecular Velcro' type in wood under mechanical stress. *Journal of Theoretical Biology*, *253*, 434-445.
- Bergander, A., & Salmén, L. (2002). Cell wall properties and their effects on the mechanical properties of fibers. *Journal of Materials Science*, *37*, 151-156.
- Cave, I. D. (1968). The anisotropic elasticity of the plant cell wall. *Wood Science and Technology*, *2*, 268-278.
- Chen, Q., & Schmidt-Rohr, K. (2006). Measurement of the local  $^1\text{H}$  spin-diffusion coefficient in polymers. *Solid State Nuclear Magnetic Resonance*, *29*, 142-152.
- Clauss, J., Schmidt-Rohr, K., & Spiess, H. W. (2003). Determination of domain sizes in heterogeneous polymers by solid-state NMR. *Acta Polymerica*, *44*, 1-17.
- Cowdrey, D. R., & Preston, R. D. (1965). The mechanical properties of plant cell walls: helical structure and Young's modulus of air-dried xylem in *Picea sitchensis*. In W. A. Côté (Ed.), *Cellular Ultrastructure of Woody Plants*. (pp 475-492), New York: Syracuse University Press.
- Cowdrey, D. R., & Preston, R. D. (1966). Elasticity and microfibrillar angle in the wood of Sitka spruce. *Proceedings of the Royal Society B*, *166*, 245-272.
- Donaldson, L. (2007). Cellulose microfibril aggregates and their size variation with cell wall type. *Wood Science and Technology*, *41*, 443-460.
- Frey-Wyssling, A. (1968). The ultrastructure of wood. *Wood Science and Technology*, *2*, 73-83.
- Gravitis, J. (2006). Nano level structures in wood cell wall composites. *Cellulose Chemistry and Technology*, *40*, 291-298.
- Hansen, C.M., & Björkman, A. (1998). The ultrastructure of wood from a solubility parameter point of view. *Holzforschung*, *52*, 335-344.
- Keckes, J., Burgert, I., Frühmann, K., Müller, M., Kölln, K., Hamilton, M., Burghammer, M., Roth, S., V., Stanzl-Tschegg, S., & Fratzl, P. (2003). Cell-wall recovery after irreversible deformation of wood. *Nature Materials*, *2*, 810-814.
- Klauditz, W., Marschall, A., & Ginzel, W. (1947). Zur Technologie verholzter pflanzlicher zellwände. *Holzforschung*, *1*, 98-103.
- Kretschmann, D. (2003). Velcro mechanics in wood. *Nature Materials*, *2*, 775-776.
- Laffend, K. B., & Swenson, H. A. (1968). Effect of acetyl content of glucomannan on its sorption onto cellulose and on its beater additive properties. *Tappi*, *51*(3), 118-123.
- Mark, R. (1965). Tensile stress analysis of the cell walls of coniferous tracheids. In W. A. Côté (Ed.), *Cellular Ultrastructure of Woody Plants* (pp 493-533). New York, USA: Syracuse University Press.
- McBrierty, V. J. (1979). Heterogeneity in polymers as studied by nuclear magnetic resonance. *Faraday Discussions of the Chemical Society*, *68*, 78-86.
- Newman, R. H. (1987). Effect of finite preparation-pulse power on carbon-13 cross-polarisation NMR spectra of heterogeneous samples. *Journal of Magnetic Resonance*, *72*, 337-340.
- Newman, R. H. (1991). Proton spin diffusion monitored by  $^{13}\text{C}$  NMR. *Chemical Physics Letters*, *180*, 301-304.

- Newman, R. H. (1992). Nuclear magnetic resonance study of spatial relationships between chemical components in wood cell walls. *Holzforschung*, 46, 205-210.
- Newman, R. H., & Hemmingson, J. A. (1998). Interactions between locust bean gum and cellulose characterized by  $^{13}\text{C}$  n.m.r. spectroscopy. *Carbohydrate Polymers*, 36, 167-172.
- Nomura, T., & Yamada, T. (1972). Structural observation on wood and bamboo by X-ray. *Wood Research*, 52, 1-12.
- Page, D. H. (1976). A note on the cell-wall structure of softwood tracheids. *Wood Fiber*, 7, 246-248.
- Ruel, K., Barnoud, F., & Goring, D. A. I. (1978). Lamellation in the S2 layer of softwood tracheids as demonstrated by scanning transmission electron microscopy. *Wood Science and Technology*, 12, 287-291.
- Salmén, L., & Fahlen, J. (2006). Reflections on the ultrastructure of softwood fibers. *Cellulose Chemistry and Technology*, 40, 181-185.
- Schmidt-Rohr, K., Clauss, J., Blümich, B., & Spiess, H. W. (1990). Miscibility of polymer blends investigated by  $^1\text{H}$  spin diffusion and  $^{13}\text{C}$  NMR detection. *Magnetic Resonance in Chemistry*, 28, S3-S9.
- Sedighi-Gilani, M., & Navi, P. (2007). Experimental observations and micromechanical modelling of successive-damaging phenomenon in wood cells' tensile behaviour. *Wood Science and Technology*, 41, 69-85.
- Takeda, F., Koshijima, T., & Okamura, K. (1981). Characterization of cellulose in compression and opposite woods of a *Pinus densiflora* tree grown under the influence of strong wind. *Wood Science and Technology*, 15, 265-273.
- Tekely, P., Canet, D., & Delpuech, J.-J. (1989). Observation of  $^1\text{H}$  nuclei in heterogeneous solids via cross-polarization  $^{13}\text{C}$  N.M.R. *Molecular Physics*, 67, 81-96.
- Weatherwax, R. C. (1974). Transient pore structure of cellulosic materials. *Journal of Colloid and Interface Science*, 49, 40-47.